Transitional granulite–eclogite facies metamorphism of basic supracrustal rocks in a shear zone complex in the Precambrian shield of south India

Biswajit Mukhopadhyay

Department of Geological Sciences, Southern Methodist University, Dallas, Texas 75275, U.S.A.

AND

Mihir K. Bose

Department of Geology, Presidency College, Calcutta 700073, India

Abstract

The phase petrology of two bodies of basic granulites occurring in association with supracrustal sequences within a dextral oblique-slip shear complex in the high-grade terrain of south India, have been studied. Some metabasites are characterized by garnet + clinopyroxene assemblages such as Grt + Cpx + Pl $\pm$ Hbl $\pm$ Opx $\pm$ Qtz + Fe–Ti oxide(s) which are high-pressure granulites (garnet–clinopyroxene subfacies) transitional between the intermediate-pressure granulites (orthopyroxene–plagioclase subfacies) and eclogite. Mineralogical characteristics suggest that metamorphic conditions did not reach the eclogite facies but certainly approached that level. Close spatial association of the garnetiferous varieties with garnet-free assemblages (Opx + Hbl + Pl $\pm$ Cpx) and intimate juxtaposition of anhydrous and hydrous assemblages indicate a complex interplay of variable μ_{H_2O} and bulk composition, especially a_{SiO_2}. Due to variable and low closure temperature of Fe–Mg exchange reactions between coexisting pyroxene and garnet, a reliable estimation of peak temperatures during this near eclogite-facies metamorphism is problematic. A combination of a garnet-clinopyroxene barometer and various temperature estimates suggests P–T conditions of 875 $\pm$ 25°C and 8 $\pm$ 1 kbar for the Mettuppalaiyam samples and 900 $\pm$ 50°C and 14 $\pm$ 2 kbar for the Kanjamalai samples. Bulk rock chemical differences in terms of SiO_2-content can account for the development of similar mineral assemblages along a near adiabatic metamorphic gradient between these two localities. These assemblages represent some of the highest grade granulite facies rocks in south India. The high-pressure granulites are not *in situ* samples of ancient lower continental crust, but low-pressure protoliths buried at depth. Textural features suggest that the high-pressure garnet–clinopyroxene subfacies rocks evolved from an amphibolitic assemblage by formation of garnet at the expense of hornblende and plagioclase and this high-pressure assemblage underwent an isothermal decompression indicating a clockwise P–T–t path resulting from crustal thickening and exhumation. A later isobaric cooling, possibly accompanying shearing and high H_2O influx ($a_{H_2O} \approx 0.78$) gave rise to the coexisting orthopyroxene–plagioclase subfacies rocks (intermediate pressure granulites).

KEYWORDS: metamorphism, granulite-eclogite facies, Precambrian, India

Introduction

THE charnockites and associated granulites from the high-grade Precambrian terrain of south India have received considerable attention over the years (e.g. Howie, 1955; Subramanium, 1959; Condie *et al.*, 1982; Harris *et al.*, 1982; Bhattacharya and Sen, 1986; Newton and Hansen, 1986). The mafic granulites associated with the charnockites typically contain an equilibrium assemblage of Opx + Cpx + Pl + Hbl + accessory minerals $\pm$ Grt $\pm$ Bt (abbreviations are after Kretz, 1983) but the garnetiferous varieties are extremely rare (Ray, 1970; Ray and Sen, 1970; Sen, 1973; Sen and Ray,
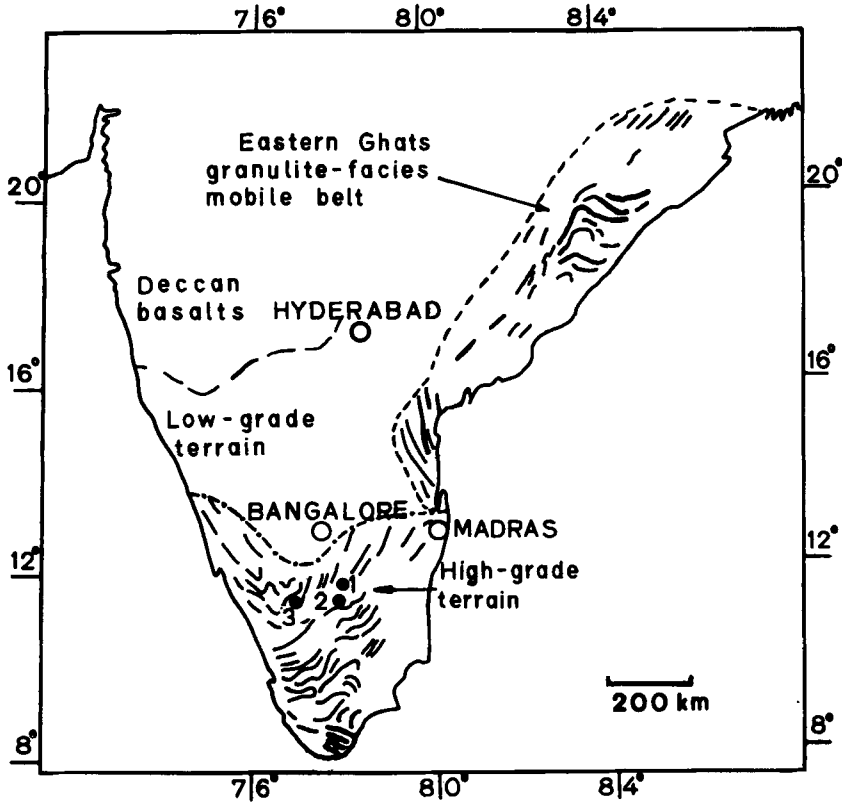
FIG. 1. Generalized map showing the high-grade (granulite-facies) terrain of south India (the different provinces are drawn after Naqvi and Rogers, 1987) and locations (solid dots) of Kanjamalai (1), Sittampundi (2), and Mettuppalaiyam (3). The high-grade terrain of south India is separated from the low-grade (granite-greenstone) terrain by an orthopyroxene isograd (dashed-dotted line). The Eastern Ghats mobile belt is considered to be a separate granulite-facies terrain (Naqvi and Rogers, 1987). Structural trends in both the granulite-facies terrains are drawn after Bose (1979). Locations of three major cities in south India are shown by open circles.

1971 a, b; Weaver et al., 1978; Janardhan et al., 1982; Rath et al., 1983). Apart from these mafic granulites, some metabasites are either associated with deformed igneous complexes or form patches and tracts, structurally conformable to the gneissic-pelitic country rocks and are commonly associated with banded iron formations (Windley and Selvan, 1975; Subba Reddy and Prasad, 1982; Naqvi and Rogers, 1987). These basic granulites contain Grt + Cpx $\pm$ Opx $\pm$ Pl $\pm$ Hbl $\pm$ Fe–Ni oxides. These assemblages are of particular interest in a granulite facies environment because they can be viewed as transitional to eclogite facies. Such an 'eclogitic' (Grt + Cpx $\pm$ Pl $\pm$ Opx $\pm$ Hbl) was reported by Subramaniam (1956)

from the metamorphosed anorthositic igneous complex of Sittampundi, in the Salem district of Tamil Nadu state. Similar granulite-facies Grt + Cpx $\pm$ Pl parageneses have also been described from South Harris, Scotland (Davidson, 1943; Livingstone, 1967; Wood, 1975). De Waard (1965a) noted almandine–clinopyroxene-bearing assemblages in rocks of diverse composition within proximity of anorthosite massifs from the granulite facies terrain of the Adirondack Highlands. This led De Waard (1965b) to advocate a six-fold subdivision of silica-saturated granulite facies rocks based on P_{Total}–P_{H_2O}–T conditions. Quartz-saturated rocks with stable orthopyroxene belong to the low-pressure ortho-
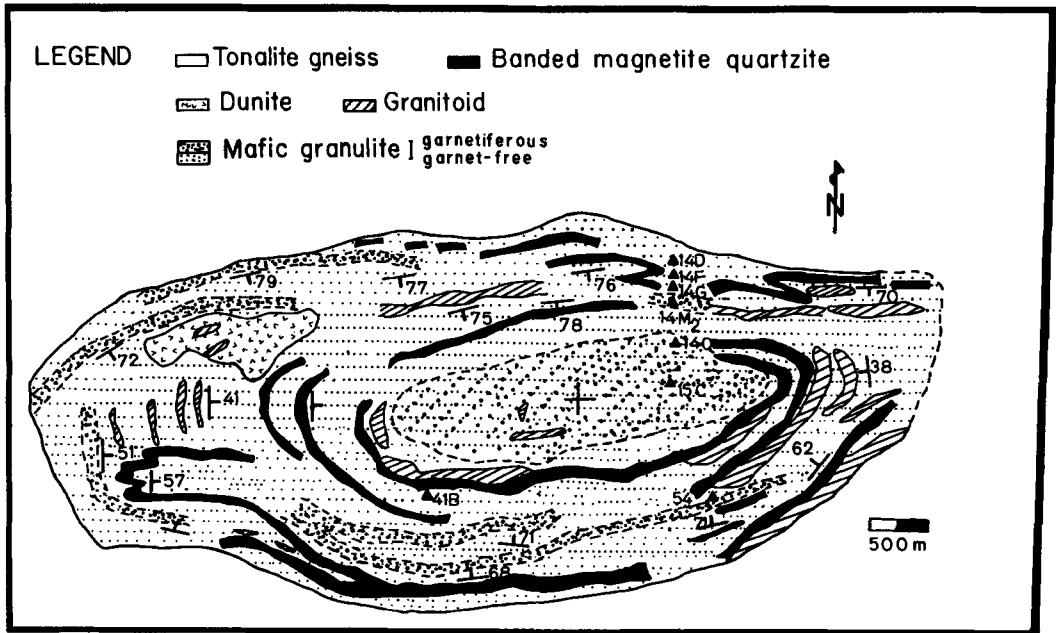
FIG. 2. Geological map of basic granulites associated with BMQ near the Kanjamalai village. Locations of the samples studied (Table 1) are shown by triangles.

pyroxene–plagioclase subfacies, whereas quartz-saturated rocks with coexisting garnet and clinopyroxene belong to the high-pressure clinopyroxene–almandine subfacies. Depending on P_{H_2O}, hornblende may be present in either of these two characteristic assemblages (De Waard, 1965a,b).

Slightly to the northeast of Sittampundi ($11°14'N;77°54'E$), near Kanjamalai ($11°37'N;78°05'E$) in the Salem district of Tamil Nadu state, occurs a deformed sequence of banded magnetite-quartzite (BMQ) inter-layered with basic granulites. A similar lithologic assemblage is also found near Mettuppalaiyam ($11°18'N;76°56'E$) in the Coimbatore district of Tamil Nadu (Fig. 1). The lithologic association of mafic granulites with BMQ at Kanjamalai and Mettuppalaiyam is similar to that observed in the Sittampundi complex, though anorthositic assemblages are absent in the former areas. Thus, the metabasites such as, garnet-granulites ('eclogites') and two-pyroxene granulites of the Sittampundi complex imply a regional distribution. Interestingly, the garnetiferous and non-garnetiferous assemblages of mafic granulites, developed in two distinct situations, as mentioned earlier, are found in close spatial association in the Kanjamalai complex and demand closer atten-

tion. Locally the garnetiferous type is essentially a garnet + clinopyroxene-bearing assemblage. Saravanan (1960) called these rocks 'eclogites of Kanjamalai'. Similarly, Viswanathan (1969) described the occurrence of those mafic granulites near Mettuppalaiyam as 'rocks of eclogitic character'. In this paper we discuss the phase petrology of the mafic granulites from the Kanjamalai and Mettuppalaiyam areas in order to decipher the metamorphic evolution of these 'eclogitic' assemblages in a granulite-facies environment.

Geological setting

The low-grade (granite–greenstone) terrain of the Precambrian shield of south India grades southward into the high-grade (granulite–charnockite) terrain (Fig. 1). The areas of the present investigation are situated within this high-grade terrain which comprised dominantly granitic gneisses, khondalites, leptynites, charnockites, metabasites, calc-silicate rocks, banded iron formations, and deformed (often metamorphosed) igneous intrusives such as anorthosite-gabbro complexes and late alkaline igneous complexes (Naqvi and Rogers, 1987).

TABLE 1. Phase assemblages in the mafic granulites from Mettuppalaiyam-Kanjamalai areas [t = trace amount; m = minor amount]

Sp. No.	Assemblages	Texture	Remarks
A. Mettuppalaiyam area			
40	Grt + Opx + Qtz + Ilm	Coarse, equigranular, polygonal, granoblastic	Cpx- and Pl-free anhydrous assemblage. Opx is often altered.
P92C	Grt + Cpx + Pl [m] + Ilm + Mag	Equigranular, polygonal granoblastic mosaic of Grt and Cpx with smaller grains of interstitial Pl.	Secondary amphibole present; Grt contains very minor inclusions of Pl. Nearly approaching eclogitic assemblage.
6D	Grt + Cpx + Pl + Opx [m] + Ilm + Mag	Inequigranular, polyganol granoblastic Pl-Cpx-Opx and Cpx-Grt-Pl are in local equilibrium.	Proportion of plagioclase, occurring as interstitial grains, is considerably higher than that in P92C. Pl contains inclusions of Cpx.
Pl09	Grt + Cpx + Pl + Hbl + Ilm	Inequigranular, interlobate to polygonal granoblastic; Hbl engulfs Cpx and Pl.	A blue amphibole, occurring in disequilibrium with cpx, is secondary.
36M	Grt + Cpx + Opx [m] + Hbl + Pl [t]	Inequigranular, interlobate granoblastic; a crude banding is developed.	Primary brown Hbl occurs as interstitial grains and includes Cpx; Grt contains minor inclusions of Hbl, Pl, and Cpx. Secondary amphibole is also present.
D87	Grt + Cpx [m] + Opx + Hbl + Pl [t] + Mag	Equigranular, polygonal granoblastic	Grt contains inclusions of Pl and Cpx.
P84	Opx + Cpx + Hbl [t] + Pl [m]	Coarse, equigranular, polygonal granoblastic. Hbl occurs only in a restricted portion.	The nongarnetiferous facies of the banded mafic granulites. Hbl includes Opx and Pl.
B. Kanjamalai area			
14/O	a) Grt + Cpx + Pl [t] b) Grt + Cpx + Opx [t]	Coarse, inequigranular, granoblastic. Opx bearing portion is very localized in a portion	Grt forms kelyphitic rims around Pl. Nearly approaching eclogitic assemblage.
15/C	Grt + Cpx + Hbl + Pl + Qtz [t] + Ilm [t]	Inequigranular, interlobate, granoblastic. Cpx-Pl-Hbl rich portion grades into Grt-rich ponion.	Grt is sieved containing inclusions of Pl, Cpx, Hbl, and Qtz; Grt often forms rims around Pl. Hbl contains no inclusion.
14/M2	Grt + Cpx + Opx + Hbl + Pl + Qtz + Ilm + Rt	Inequigranular, interlobate, granoblastic. Grt is very sieved.	Cpx and Pl predate Grt by having Grt rims around. Hbl contains inclusions of Opx and rarely Grt.
54	a) Grt + Opx + Cpx + Hbl + Pl + Ilm [t] b) Opx + Cpx + Hbl + Pl.	Equigranular, polygonal; garnet rich layers form banding. Grt-bearing portion grades into Grt-free portion.	Hbl contains abundant inclusions of Opx, Pl and Ilm; while Grt contains inclusions of Hbl.
14/G	Opx + Hbl + Pl [m]	Slightly inequigranular, granoblastic	Subhedral Hbl poikilitically encloses rounded Opx and Pl. Nongarnetiferous facies.
14F	Opx + Hbl + Pl + Ilm	Inequigranular, granoblastic	Hbl contains abundant inclusions of Opx and Pl. Nongarnetiferous facies.
14/D	Opx + Hbl + Pl + Ilm	Similar to 14/F	Nongarnetiferous facies
41/B	Hbl + Spl + Pl(t) + Ilm + Mag	Inequigranular granoblastic polygonal	Grt-free, pyroxene-free sample (amphibolite). Rounded spinel enclose Fe-Ti oxide. Pl occurs as minor interstitial grains.

At Kanjamalai Hill (6 km SW of Salem) a complex, surrounded by tonalitic gneisses, is made up of BMQ layers alternating with metabasic bands and deformed lenses of granitoid (Fig. 2). The rocks have undergone three phases of folding with two distinct structural closures. The east–west trending axial plane conforms to the regional synform. The metabasic bands reveal two petrographic types, *viz.* garnetiferous varieties with occasional crude banding and garnet-free, weakly-foliated varieties. An intimate spatial association often limits clear delineation of the two types (Fig. 2). To the east of Mettuppalaiyam, a similar complex consisting of BMQ and mafic granulites forms a narrow tight synformal fold with distinct closure to the east and an E–W axial trend. Here also, two petrographic types of granulites, *viz.* garnetiferous and non-garnetiferous, are developed, but the former occasionally grade to garnet pyroxenites ('eclogite') and are relatively more abundant. The three localities mentioned above, *viz.*, Sittampundi, Kanjamalai, and Mettuppalaiyam, are all confined within the E–W trending Moyar–Bhavani and Noyil–Cauvery shear systems (Fig. 10, discussed later). These two shear zones together form a dextral oblique-slip shear complex of Proterozoic supracrustal sequences (Drury and Holt, 1980; Mukhopadhyay, 1986).

Phase assemblages

Two distinct petrographic variants of the mafic-ultramafic bands are recognized. These are: (1) Grt
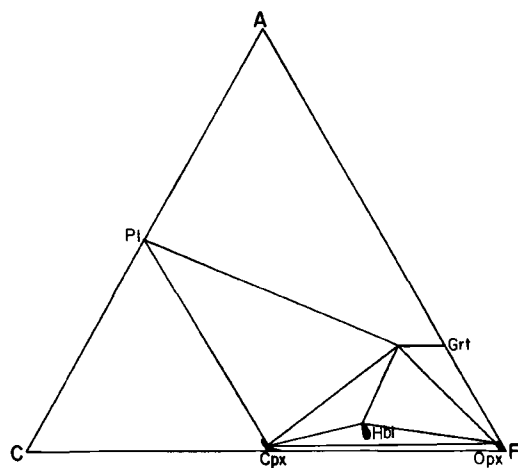

FIG. 3. ACF diagram showing possible compatibility relations of coexisting plagioclase, clinopyroxene, orthopyroxene, garnet, and hornblende.

+ Cpx + Pl $\pm$ Opx $\pm$ Hbl $\pm$ Ilm $\pm$ Mag (garnet-clinopyroxene subfacies); and (2) Opx + Pl + Hbl $\pm$ Cpx + Ilm (orthopyroxene-plagioclase subfacies). Several other minor petrographic variants are also found (Table 1). The most conspicuous assemblage is the five-phase assemblage Grt + Cpx + Opx + Pl + Hbl. The role of the oxides which are ubiquitous, can be treated as an independent subsystem. Proportions of individual silicate phases vary to such an extent that certain phases are completely absent in places (Table 1). This variation can be noted even on the scale of a thin section. Free quartz was noted in some samples and hence the rocks are, in general, considered to be just silica saturated. Some possible phase relations are illustrated with an ACF diagram (Fig. 3). The most common five-phase assemblage represents the equilibrium assemblage with minimum thermodynamic variance. The assemblages with the highest thermodynamic degree of freedom are various combinations of three-phase assemblages such as those shown in Fig. 3. Of all the possible three-phase assemblages, two are quite obvious. These are Grt + Cpx + Pl and Opx + Pl + Hbl assemblages, belonging to the garnet–clinopyroxene and orthopyroxene–hornblende–plagioclase subfacies (De Waard, 1965*b*) respectively. Although no biminerallic Grt + Cpx-bearing sample was found in our collection, their presence can be predicted from Fig. 3. For example, at Sittampundi a biminerallic garnet + clinopyroxene-bearing rock has been recognized (Chappel and White, 1970). Similarly, Viswanathan (1969) described one rock (Sp. No. 198/68) containing 68.2% Grt, 30.3% Cpx, 0.7% Opx, and 0.8% secondary minerals as an 'eclogite' from Mettuppalaiyam. In the anhydrous assemblage from Kanjamalai (Sp. 14/O), plagioclase only occurs as inclusions within garnet grains indicating a near eclogite-facies assemblage.

Phase chemistry

Minerals were analysed with a JEOL 733 Superprobe with Krisel automation. The accelerating potential was 15 kV, beam current was 20 nA and the beam-diameter was 10 μm. Several spots on the same grain were first analysed to check the homogeneity of the phase thoroughly, and then several grains of the same phase were analysed in the same polished-section. An individual analysis, reported here, is an average of 10–12 such spot analyses.

Clinopyroxene. Compositions of clinopyroxenes (Table 2), in general, are dominated by the

TABLE 2. Clinopyroxene compositions.

| | Mettuppalaiyam Area | | | | | | | | Kanjamalai Area | | | |
	P92C	36M	P109	6D	D87	P94	29F		14M2	14/O	15/C	54
SiO_2	51.41	51.81	52.26	51.71	51.90	51.87	52.18		53.86	52.51	52.76	53.14
TiO_2	0.55	0.47	0.64	0.47	0.31	0.40	0.26		0.19	0.25	0.38	0.29
Al_2O_3	4.72	4.32	5.17	4.90	6.16	5.05	3.24		2.47	4.84	3.48	3.30
Cr_2O_3	0.04	0.17	0.05	0.08	0.13	0.61	0.03		0.06	0.26	0.07	0.05
FeO	8.67	5.82	6.38	8.07	6.59	6.22	6.75		7.47	5.06	8.13	8.38
MnO	0.08	0.09	0.04	0.08	0.04	0.14	0.03		0.12	0.12	0.07	0.24
MgO	12.22	13.76	12.99	12.19	12.59	13.19	13.34		13.40	14.17	12.54	12.76
CaO	21.46	22.31	21.88	21.70	21.13	22.11	21.93		21.77	23.23	21.45	21.27
Na_2O	1.10	0.96	1.22	1.01	1.24	0.90	0.91		0.66	0.04	0.79	0.70
Σ	100.25	99.71	100.63	100.21	100.09	100.49	98.67		100.01	100.48	99.67	100.11

Structural formulae on the basis of Σ cations = 4

Si	1.903	1.908	1.911	1.914	1.907	1.903	1.950		1.997	1.927	1.968	1.974
Al^{IV}	0.097	0.092	0.089	0.086	0.093	0.097	0.050		0.003	0.073	0.032	0.026
Ti	0.015	0.013	0.018	0.013	0.009	0.011	0.007		0.005	0.007	0.011	0.008
Cr	0.001	0.005	0.001	0.002	0.004	0.018	0.001		0.002	0.008	0.002	0.002
Al^{VI}	0.109	0.096	0.133	0.127	0.174	0.122	0.093		0.105	0.136	0.121	0.119
F^{2+}	0.268	0.179	0.195	0.250	0.202	0.191	0.211		0.231	0.155	0.253	0.260
Mn	0.002	0.003	0.001	0.002	0.001	0.004	0.001		0.004	0.004	0.002	0.008
Mg	0.674	0.755	0.708	0.672	0.690	0.721	0.743		0.740	0.775	0.697	0.707
Ca	0.851	0.880	0.857	0.860	0.832	0.869	0.878		0.865	0.913	0.857	0.847
Na	0.079	0.069	0.087	0.073	0.088	0.064	0.066		0.047	0.003	0.057	0.050

TABLE 3. Orthopyroxene compositions.

| | Mettuppalaiyam Area | | | | | | Kanjamalai Area | | | | | |
	6D	D87	P84	36M	40		14/O	14M2	54	14/G	14/D	14/F
SiO_2	52.04	53.63	52.47	52.39	50.61		53.77	52.30	51.90	53.45	52.05	52.04
TiO_2	0.04	0.04	0.04	0.05	0.05		0.04	0.04	0.07	0.03	0.07	0.16
Al_{2O_3}	2.91	3.28	3.56	2.16	0.45		3.23	2.12	2.00	2.50	1.86	2.46
Cr_2O_3	0.05	0.05	0.34	0.10	0.04		0.20	0.03	0.01	0.13	0.05	0.08
FeO	22.49	16.79	18.07	19.34	35.40		13.95	25.56	25.05	17.71	25.55	21.41
MnO	0.21	0.17	0.36	0.22	0.12		0.23	0.61	0.59	0.41	0.79	0.45
MgO	22.03	26.30	24.86	24.56	13.96		27.85	19.64	19.76	25.63	19.96	22.92
CaO	0.31	0.20	0.30	0.39	0.46		0.26	0.36	0.39	0.27	0.58	0.29
Na_2O	0.01	0.01	0.02	0.02	0.01		0.01	0.01	0.01	0.00	0.02	0.01
Σ	100.11	100.47	100.02	99.23	101.10		99.54	100.68	99.78	100.31	100.93	99.80

Structural formulae on the basis of Σ cations = 4

Si	1.933	1.930	1.912	1.932	1.981		1.930	1.966	1.965	1.941	1.950	1.930
Al^{IV}	0.067	0.070	0.008	0.068	0.019		0.070	0.034	0.035	0.059	0.050	0.070
Ti	0.001	0.001	0.001	0.001	0.002		0.001	0.001	0.002	0.001	0.002	0.004
Cr	0.002	0.001	0.010	0.003	0.001		0.006	0.001	0.000	0.004	0.002	0.002
Al^{VI}	0.060	0.069	0.065	0.026	0.002		0.067	0.060	0.055	0.048	0.032	0.037
Fe^{2+}	0.698	0.505	0.550	0.596	1.157		0.418	0.803	0.792	0.537	0.800	0.663
Mn	0.007	0.005	0.011	0.007	0.004		0.007	0.019	0.019	0.013	0.025	0.014
Mg	1.219	1.410	1.350	1.350	0.814		1.490	1.100	1.115	1.387	1.115	1.267
Ca	0.012	0.008	0.012	0.015	0.019		0.010	0.015	0.016	0.011	0.023	0.011
Na	0.001	0.001	0.001	0.001	0.001		0.001	0.001	0.000	0.000	0.001	0.001

quadrilateral components, having Q:J > 4:1 (see Morimoto *et al.*, 1988). The clinopyroxenes are mostly diopside–hedenbergite solutions with a limited range of Mg # [$100Mg/(Mg + Fe^{2+})$] = 72–83. No zoning was observed within an individual grain. Alteration of clinopyroxenes to secondary blue amphibole along the grain boundaries, is common.

Eclogitic clinopyroxenes are enriched in non-quadrilateral components (J), particularly jadeite (Jd) and aegirine (Ae). Enrichment of non-quadrilateral components in pyroxenes can result not only from Jd and Ae components, but also from Tschermak (Ts) components. The complexity of pyroxenes rich in non-quadrilateral components results from coupled substitution of divalent and tetravalent cations by monovalent and trivalent cations in the $M1$, $M2$, and T sites (Cameron and Papike, 1979). Two distinct trends are possible: the

diopside–omphacite–aegerine trend and the diopside–Tschermak substitutions trend. These can be illustrated by a set of exchange vectors with diopside as the additive component as shown below.

$$CaMgSi_2O_6 \rightarrow$$

$$(NaCa_{-1})^{M2} + (R^{3+}R^{2+}_{-1})^{M1}$$
[jadeite, aegirine, kosmochlor]

$$(R^{3+}R^{2+}_{-1})^{M1} + (AlSi_{-1})^{T}$$
[Ca-, CaFe^{3+}-, Cr- Tschermak]

$$(R^{4+}R^{2+}_{-1})^{M1} + (AL_2Si_{-2})^{T}$$
[Ti- Tschermak]

The various end-member components were calculated following the method described by Lindsley and Anderson (1983). As shown above, Fig. 4 shows the relative proportions of total

FIG. 4. Compositions of clinopyroxenes in terms of quadrilateral (QUAD) components, Tschermak (TS) component, and jadeite (JD) component. JD:TS = 1:2 reference line was used by Lovering and White (1969) to separate clinopyroxenes of eclogite-facies from those of granulite facies environment [triangles = Kanjamalai samples; circles = Mettuppalaiyam samples].
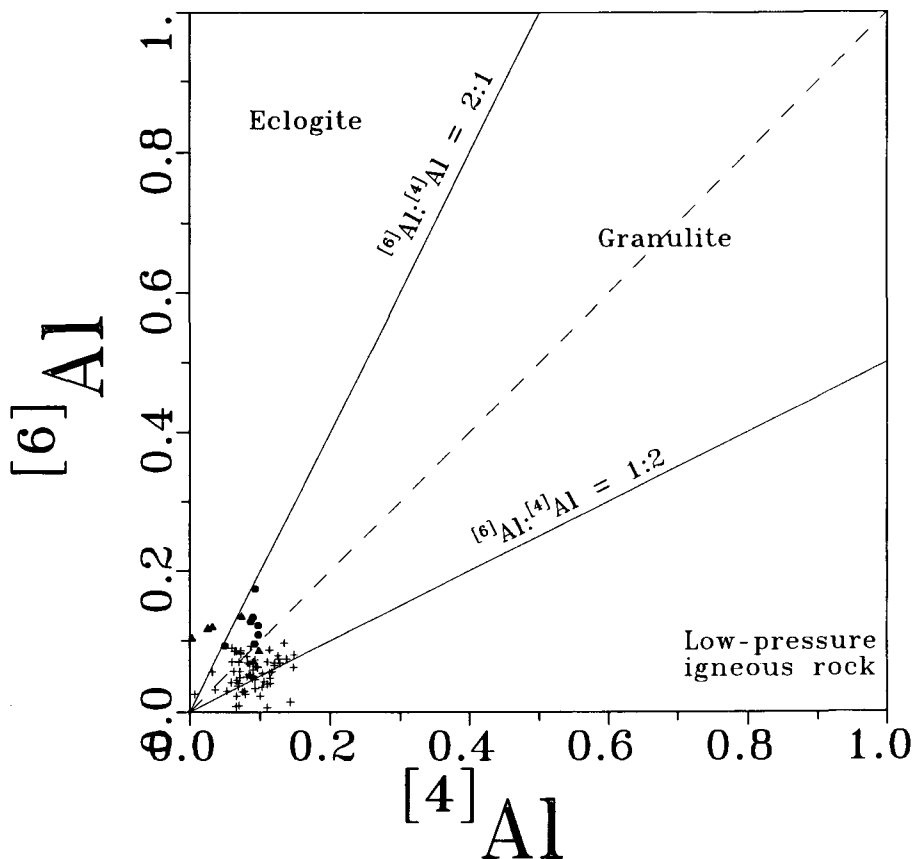
FIG. 5. [6]Al vs. [4]Al plots of the clinopyroxenes from mafic granulites of the Mettuppalaiyam–Kanjamalai areas (symbols are same as in Fig. 4) and those associated with charnockites (crosses). The data for the latter categories are from Weaver et al. (1978), Ray and Sen (1970), Raith et al. (1983) and Janardhan et al. (1982)

quadrilateral components (Q), jadeite (JD) and total tschermak (TS) components. Lovering and White (1969) used a similar diagram and showed that eclogitic clinopyroxenes are more enriched in JD relative to the TS, whereas for the granulite-facies clinopyroxenes the reverse holds true. Since clinopyroxene composition space is a complex reciprocal space, calculation of the end-member components is an arbitrary procedure. However, the relative enrichment in JD and TS components can possibly be evaluated from a plot (Fig. 5) of [6]Al versus [4]Al (Mukhopadhyay, 1991). These diagrams suggest that although these clino-pyroxenes possess compositional characteristics of granulite facies clinopyroxenes, they actually exhibit a gradation toward the characteristics of the eclogite facies clinopyroxenes.

Orthopyroxene. Orthopyroxenes (Table 3) are either hypersthene (Mg # = 58–70) or bronzite (Mg # = 71–78), except in Sp. 40 (Opx + Grt + Qtz + Ilm) in which orthopyroxene is ferro-hypersthene (Mg # = 41). In the latter sample, orthopyroxene is highly altered to orthoamphibole uniformly along the grain boundaries. In all other samples, orthopyroxenes are fresh and chemically homogeneous. The orthopyroxenes are extremely poor in Ca and thus conform to the subsolidus metamorphic trend.

Garnet. Garnet grains are compositionally quite homogeneous showing no zoning from the core to the rim of a grain. The garnets are pyrope–almandine solid solutions with minor grossular and insignificant spessartine components (Table 4). The most almandine-rich garnet is found in Sp. 40 (garnet–orthopyroxene rock). Similarly, the most pyrope-rich garnet was reported from Sp. 198/68 (essentially biminerallic garnet–clino-pyroxene rock with minor hypersthene) by

TABLE 4. Garnet compositions

	Mettuppalaiyam Area							Kanjamalai Area			
	P92C	36M	P109	6D	D87	40	29F	14M2	14/O	15/C	54
SiO_2	38.60	39.57	39.23	39.21	39.66	36.98	39.19	39.03	39.71	38.99	38.67
TiO_2	0.05	0.02	0.10	0.04	0.05	0.05	0.05	0.05	0.03	0.05	0.03
Al_2O_3	21.39	22.02	21.56	21.48	21.94	20.13	21.36	21.63	22.06	21.50	21.40
Cr_2O_3	0.04	0.18	0.08	0.02	0.08	0.29	0.06	0.11	0.11	0.04	0.03
FeO	25.21	21.40	23.05	24.68	20.40	33.33	25.10	23.95	17.68	25.77	25.87
MnO	0.67	0.62	0.49	0.69	0.51	0.29	0.63	0.59	0.86	0.64	0.83
MgO	7.57	10.20	8.80	7.68	11.03	3.86	7.33	7.94	10.44	5.79	5.98
CaO	6.60	5.66	5.96	6.42	5.78	5.13	6.23	6.84	8.84	7.93	7.56
Σ	100.13	99.67	99.27	100.22	99.45	100.07	99.95	100.15	99.73	100.71	100.37

Structural formulae on the basis of Σ cations = 4

|											
Si	2.973	3.005	3.019	3.013	3.001	2.949	3.027	2.993	2.987	3.011	2.996
Al	1.942	1.971	1.956	1.946	1.957	1.893	1.945	1.955	1.956	1.957	1.954
Ti	0.003	0.001	0.006	0.002	0.003	0.003	0.003	0.003	0.002	0.003	0.002
Cr	0.002	0.011	0.005	0.001	0.005	0.018	0.004	0.007	0.006	0.002	0.002
Fe^{2+}	1.622	1.357	1.482	1.584	1.289	2.220	1.620	1.534	1.111	1.662	1.674
Mn	0.044	0.040	0.032	0.045	0.033	0.020	0.042	0.038	0.055	0.042	0.055
Mg	0.869	1.154	10.009	0.880	1.244	0.459	0.844	0.907	1.170	0.666	0.690
Ca	0.545	0.461	0.492	0.529	0.469	0.438	0.516	0.563	0.713	0.656	0.628
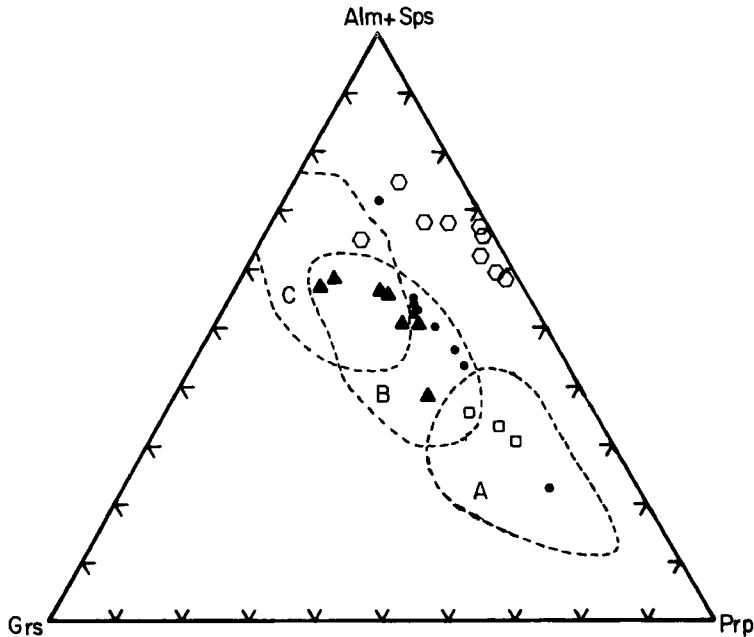
FIG. 6. Compositions of garnet in terms of atomic proportions of Ca–Mg–(Fe + Mn). Fields of eclogitic garnets (drawn after Mottana, 1986) are shown for reference. [circles = Mettuppalaiyam; triangles = Kanjamalai; squares = Sittampundi 'eclogites' (data are from Subramanium, 1957, and Chappel and White, 1970); hexagons = charnockites and associated mafic granulites of the type charnockite area near Madras (data are from Howie and Subramanium, 1957; Weaver *et al.*, 1978); Bhattacharya and Sen, 1986)]. The data on the most pyrope-rich garnet from Mettuppalaiyam are taken from Viswanathan (1969, Sp. N. 198/68).

TABLE 5. Amphibole Compositions

| | Mettuppalaiyam Area | | | | | Kanjamalai Area | | | | | |
	36M	P109	D87	P84	14M2	15/C	14/D	14/F	14/G	54	41B
SiO_2	42.73	42.73	42.69	43.49	45.63	45.54	42.91	42.91	45.76	45.71	43.67
TiO_2	1.92	2.07	1.45	1.55	1.64	1.21	1.98	2.07	0.43	1.24	0.71
Al_2O_3	13.37	13.04	14.54	13.83	12.59	11.40	12.22	13.07	11.46	12.86	15.72
Cr_2O_3	0.33	0.07	0.18	0.60	0.13	0.11	0.06	0.26	0.45	0.07	0.04
Fe_2O_3	4.53	4.96	5.33	3.09	2.26	2.60	4.51	4.25	4.51	1.78	5.95
FeO	6.70	6.88	5.40	6.53	7.91	9.34	10.91	7.81	3.99	10.21	3.05
MnO	0.09	0.05	0.04	0.10	0.04	0.04	0.26	0.12	0.13	0.09	0.14
MgO	13.55	13.31	13.74	13.69	13.32	13.40	11.25	12.61	16.13	13.25	14.91
CaO	10.80	11.13	11.16	11.14	11.18	11.08	10.86	11.49	11.78	10.66	11.53
Na_2O	2.47	2.56	2.47	1.85	1.96	1.77	2.26	2.16	1.56	1.88	1.89
K_2O	0.37	0.38	0.57	0.90	0.30	0.13	0.84	0.96	0.18	0.11	0.04
F	0.12	0.18	0.18	0.02	0.06	0.08	0.14	0.15	0.03	0.02	0.09
Cl	0.00	0.00	0.00	0.01	0.01	0.02	0.00	0.00	0.00	0.00	0.00
Σ	96.98	97.36	97.75	96.81	98.03	96.72	98.20	97.86	97.42	97.89	97.74

Structural formulae on the basis of 23 oxygens

Si	6.343	6.346	6.275	6.418	6.615	6.723	6.438	6.372	6.715	6.658	6.269
Al^{IV}	1.657	1.654	1.725	1.582	1.385	1.277	1.562	1.628	1.285	1.342	1.731
Σ^{TET}	8.000	8.000	8.000	8.000	8.000	8.000	8.000	8.000	8.000	8.000	8.000
Ti	0.214	0.231	0.160	0.172	0.179	0.134	0.223	0.231	0.046	0.136	0.077
Al^{VI}	0.683	0.629	0.794	0.824	0.766	0.707	0.599	0.660	0.655	0.867	0.930
Cr	0.039	0.008	0.021	0.070	0.015	0.013	0.007	0.003	0.051	0.008	0.004
Fe^{3+}	0.506	0.554	0.590	0.344	0.246	0.289	0.509	0.475	0.487	0.195	0.643
Fe^{2+}	0.560	0.631	0.425	0.579	0.700	0.909	1.146	0.813	0.307	0.918	0.156
Mg	2.998	2.946	3.010	3.011	3.094	2.948	2.515	2.791	3.454	2.876	3.190
Σ^{OCT}	5.000	5.003	5.000	5.000	5.000	5.000	5.000	5.000	5.000	5.000	5.000
Fe^{2+}	0.271	0.223	0.237	0.226	0.258	0.242	0.221	0.157	0.172	0.325	0.209
Mn	0.011	0.006	0.005	0.013	0.005	0.005	0.033	0.015	0.016	0.011	0.017
Ca	1.718	1.771	1.758	1.761	1.737	1.753	1.746	1.828	1.812	1.664	1.774
$\Sigma^{B \; Site}$	2.000	2.000	2.00	2.000	2.000	2.000	2.000	2.000	2.000	2.000	2.000
Na	0.707	0.733	0.701	0.525	0.547	0.504	0.653	0.617	0.435	0.527	0.527
K	0.070	0.072	0.106	0.168	0.055	0.024	0.160	0.181	0.033	0.020	0.007
$\Sigma^{A \; Site}$	0.777	0.805	0.807	0.693	0.602	0.528	0.813	0.798	0.468	0.547	0.534

Viswanathan (1969). Fig. 6 shows the compositions of garnet in relation to the compositional fields of garnet in Group A, B, and C eclogites (Mottana, 1986). It is interesting to note that the majority of the garnets from Mettuppalaiyam–Kanjamalai mafic granulites fall in the field of Group B eclogites.

Amphiboles. Compositions of primary brown amphiboles are presented in Table 5. The method proposed by Robinson *et al.* (1982) for estimating Fe^{3+} in $A_{0-1}B_2C_5T_8O_{22}(OH,F,Cl)_2$ amphiboles was employed. In this method, the sum of cations excluding Na and K is considered to be 15 and Fe^{3+} is calculated by preserving charge balance. The cations were then assigned to the different sites in the order suggested by Robinson *et al.* (1982) and Hawthorne (1983).

The amphiboles are calcic amphiboles, having $(Na + Ca)_B \geqslant 1.34$ and $Na_B = 0.0$. All amphiboles, except for one in sample 14/G, are either edenitic or pargasitic hornblende (Hawthorne, 1983). Amphibole in 14/G is magnesian hornblende because of its $(Na + K)_{A-site}$ content of 0.47. Sample 41/B, an amphibolite, contains pargasitic hornblende. A characteristic feature of the hornblende is their negligible content of F and Cl.

In the encyclopedic account of the mineralogy of amphiboles in metamorphic rocks given by Robinson *et al.* (1982), considerable details are provided on the compositional characteristics of the amphiboles in greenschist, amphibolite, blueschist, and Group C eclogite facies rocks without any notes on compositional characteristics of granulite facies amphiboles, as well as

TABLE 6. Plagioclase compositions

| | Mettuppalaiyam Area | | | | | | | Kanjamalai Area | | | | | | | |
	P92C	Pl09	36M	6D	D87 Core	D87 Rim	P84	14/O	15/C	14/M2	54 Core	54 Rim	14/G	14/D	14/F
SiO_2	58.66	58.82	57.04	57.20	55.46	57.82	57.09	43.67	55.79	56.63	48.76	54.87	48.74	59.96	57.56
TiO_2	0.03	0.02	0.12	0.01	0.00	0.03	0.02	0.00	0.00	0.00	0.03	0.00	0.00	0.03	0.00
Al_2O_3	26.54	26.14	27.03	27.44	28.04	26.36	27.91	36.90	28.42	28.54	33.48	29.02	33.64	24.99	26.70
FeO	0.08	0.07	0.03	0.13	0.09	0.29	0.07	0.04	0.08	0.18	0.11	0.41	0.04	0.07	0.05
CaO	7.04	7.28	7.76	8.96	9.31	7.65	8.74	19.27	9.81	9.29	14.62	11.17	14.28	6.67	8.61
Na_2O	7.27	7.20	6.71	6.32	5.88	6.90	6.25	0.03	5.43	5.39	2.14	3.76	2.11	7.54	6.44
K_2O	0.02	0.05	0.01	0.14	0.07	0.03	0.06	0.00	0.02	0.05	0.00	0.00	0.01	0.15	0.11
BaO	0.03	0.02	0.03	0.04	0.03	0.06	0.03	0.02	0.02	0.03	0.02	0.07	0.00	0.02	0.05
SrO	0.08	0.06	0.17	0.04	0.14	0.12	0.11	0.05	0.04	0.03	0.04	0.06	0.02	0.60	0.50
Σ	99.75	99.66	98.90	100.29	99.10	99.25	100.28	99.98	99.61	100.14	99.20	99.36	98.84	100.02	100.02
Structural formulae on the basis of 8 oxygens															
Si	2.622	2.632	2.580	2.558	2.517	2.607	2.555	2.016	2.512	2.530	2.234	2.480	2.237	2.683	2.588
Ti	0.001	0.001	0.004	0.000	0.000	0.001	0.001	0.000	0.000	0.000	0.001	0.000	0.000	0.001	0.000
Al	1.399	1.379	1.441	1.447	1.500	1.401	1.470	2.008	1.508	1.503	1.808	1.546	1.820	1.318	1.415
Fe	0.003	0.003	0.001	0.005	0.003	0.011	0.003	0.001	0.003	0.007	0.004	0.016	0.002	0.003	0.002
Ca	0.337	0.349	0.376	0.429	0.453	0.370	0.418	0.953	0.473	0.445	0.718	0.541	0.702	0.320	0.415
Na	0.630	0.625	0.588	0.548	0.517	0.603	0.541	0.003	0.474	0.467	0.190	0.330	0.188	0.654	0.562
K	0.001	0.003	0.001	0.008	0.004	0.002	0.003	0.000	0.001	0.003	0.000	0.000	0.000	0.009	0.006

amphiboles in Group B eclogites. Group B eclogitic amphiboles are generally sodic, containing substantial proportions of Na in the B-site ($M4$) (e.g. see Jamtveit, 1987) Sen and Ray (1971a,b) attempted to demonstrate that granulite facies hornblendes are almost a 50:50 mixture of edenite and Tschermakite end-members and do not belong to the pargasite–ferrohastingsite series
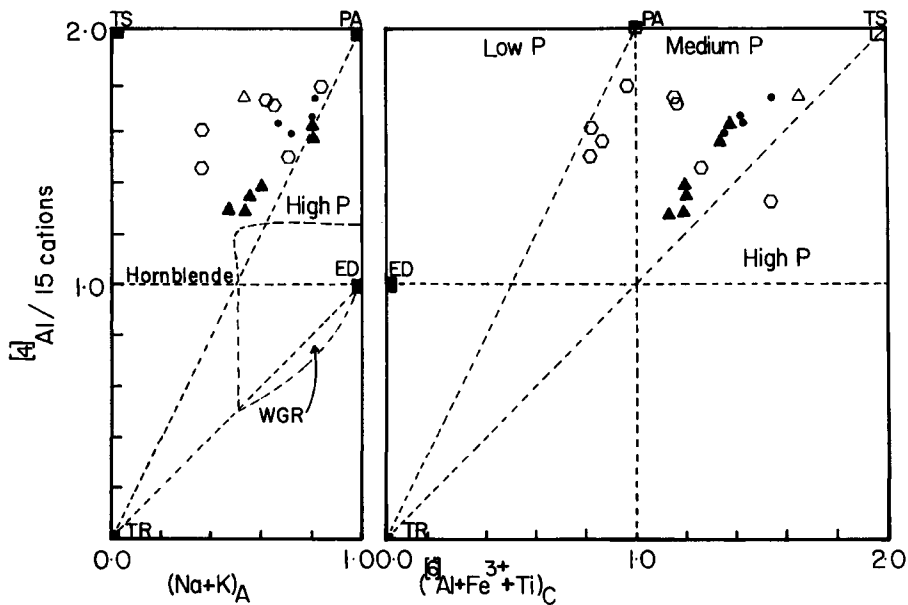
FIG. 7. Plots of $^{[4]}Al$ vs. A-site occupancy and $^{[4]}Al$ vs. $\Sigma(R^{3+} + R^{4+})$ in the $M1$-site for three groups of amphiboles: solid dots = Mettuppalaiyam samples; triangles = Kanjamalai samples; hexagons = mafic granulites associated with charnockites (see text for sources of data). The regions of high-, medium-, and low-P amphiboles are indicated from the compilations of Robinson et al. (1982). The area marked as WGR refers to the amphiboles from the western gneiss region of Norway (see text for explanation).

TABLE 7. Compositions of oxides (Note: Fe^{3+} calculated from stoichiometry. Ilm^R indicates ilmenite rim on rutile core and * indicates rutile is also present.)

	Mettuppalaiyam Area							Kanjamalai Area									
	P92C*		P109	D87	6D		40	15/C	14/M2			54	14/D	14/F		41	
	Ilm	Mag	Ilm	Mag	Ilm	Mag	Ilm	Ilm	Rt	Ilm^R	Ilm	Ilm	Ilm	Ilm	Mag	Ilm	Spl
SiO_2	0.05	0.07	0.01	0.09	0.04	0.09	0.02	0.02	0.04	0.04	0.06	0.00	0.07	0.07	0.05	0.02	0.00
TiO_2	50.27	1.12	51.01	0.12	50.05	0.22	51.39	50.72	98.73	51.61	49.45	50.35	49.72	49.52	0.16	51.02	0.00
Al_2O_3	0.03	0.21	0.04	0.36	0.05	0.35	0.03	0.07	0.06	0.01	0.07	0.05	0.07	0.04	0.39	0.04	61.27
Cr_2O_3	0.02	0.27	0.05	0.89	0.02	0.30	0.07	0.09	0.13	0.06	0.09	0.05	0.03	0.15	0.21	0.03	0.34
Fe_2O_3	4.66	32.15	4.04	67.21	5.15	67.53	2.51	4.24	-	3.14	6.90	5.74	6.25	6.22	68.61	6.00	4.38
FeO	42.53	66.74	43.06	30.89	42.01	30.71	45.37	42.93	0.41	42.77	41.03	42.33	42.56	41.66	31.05	37.92	19.09
MnO	0.24	0.02	0.27	0.02	0.22	0.06	0.09	0.08	0.01	0.15	0.20	0.20	0.80	0.66	0.10	3.15	0.34
Mgo	1.19	0.07	1.33	0.11	1.47	0.13	0.45	1.48	0.02	1.84	1.79	1.52	0.78	1.27	0.16	2.56	14.53
CaO	0.32	0.18	0.18	0.22	0.20	0.33	0.02	0.03	0.22	0.24	0.13	0.07	0.07	0.06	0.20	0.22	0.01
Σ	99.30	100.83	99.99	99.91	99.21	99.72	99.96	99.66	99.62	99.86	99.72	100.31	100.35	99.65	100.93	100.95	99.95
O≡	3	4	3	4	3	4	3	3	2	3	3	3	3	3	4	3	4
Si	0.001	0.003	0.003	0.003	0.001	0.004	0.001	0.001	0.001	0.001	0.002	0.000	0.002	0.002	0.002	0.001	0.000
Ti	0.954	0.032	0.961	0.004	0.949	0.006	0.975	0.958	0.969	0.969	0.932	0.945	0.938	0.937	0.005	0.943	0.000
Al	0.001	0.009	0.001	0.016	0.002	0.016	0.001	0.002	0.001	0.000	0.002	0.002	0.002	0.001	0.018	0.001	1.906
Cr	0.001	0.008	0.001	0.027	0.004	0.009	0.001	0.002	0.001	0.001	0.002	0.001	0.001	0.003	0.006	0.001	0.007
Fe^{3+}	0.088	1.913	0.076	1.943	0.098	1.955	0.048	0.080	-	0.059	0.130	0.108	0.118	0.118	1.963	0.111	0.087
Fe^{2+}	0.897	1.023	0.901	0.991	0.885	0.987	0.956	0.900	0.005	0.892	0.858	0.882	0.892	0.876	0.986	0.779	0.421
Mn	0.005	0.001	0.006	0.001	0.005	0.002	0.002	0.002	0.000	0.003	0.004	0.004	0.017	0.014	0.003	0.066	0.008
Mg	0.045	0.004	0.050	0.006	0.055	0.008	0.017	0.055	0.000	0.068	0.067	0.057	0.029	0.048	0.009	0.094	0.571
Ca	0.009	0.007	0.005	0.009	0.005	0.014	0.001	0.001	0.003	0.006	0.004	0.002	0.002	0.002	0.008	0.006	0.000

— a view held by various earlier workers (e.g. Ramberg, 1948). In order to evaluate such generalizations, the hornblende compositions presented here, and the hornblende compositions presented by Sen and Ray (1971) from the basic granulites associated with the type-area of charnockite, are plotted in Fig. 7. From these plots it appears that the edenite–pargasite nature of the hornblendes of basic lithologies in the granulite facies terrain of south India is a characteristic feature although a pronounced enrichment in the Tschermakitic component is evident. The Norwegian eclogitic (Group B eclogite) amphiboles, on the other hand, do not show such a distinct enrichment in Tschermakite component. This latter category of amphibole can in general be characterized by a three-component mixture of tremolite, pargasite, and edenite (Jamtveit, 1987).

Plagioclase feldspars. Plagioclase feldspars (Table 6) generally show little zonation except in samples D87 and 54. The anorthite content of plagioclase in samples from Mettuppalaiyam ranges from An_{40} to An_{60}. However, plagioclase in the samples from Kanjamalai are highly calcic (An_{70-100}), particularly in sample 14/O in which the plagioclase is almost pure anorthite indicating an effect of bulk composition.

Fe-Ti oxides and aluminous spinel. Five types of Fe-Ti oxide mineral assemblages were found. These are: (i) rutile–ilmenite–magnetite three-

phase assemblage; (ii) rutile–magnetite two-phase assemblage; (iii) magnetite–ilmenite two-phase assemblage; (iv) magnetite only; and (v) ilmenite only.

The most striking features of the Fe-Ti oxide minerals (Table 7) in all these assemblages is that the compositions are very close to those of the pure end-members with minor solubility of Mg and Mn in the ilmenites. The only sample that contains aluminous spinel is 41/B. The spinel (Table 7) is hercynitic and occurs abundantly as mantles around magnetite crystals.

Estimation of the intensive variables during metamorphism

If the coexisting phases in an assemblage reached equilibrium, its physical conditions can be estimated by various mineralogical thermometers and barometers based on systematic partitioning of elements among the phases. However, the problem of application of ion-exchange geothermometers to granulite-facies rocks has been aptly described as the 'granulite uncertainty principle' by Frost and Chacko (1989).

Temperatures are calculated (Table 8) by (i) the two-pyroxene (2-px) geothermometer (Wells 1977; Davidson and Lindsley, 1985), (ii) the garnet–clinopyroxene (grt–cpx) geothermometer (Ellis and Green, 1979; Dahl, 1980; Krogh, 1988), and (iii) the garnet–orthopyroxene (grt–opx)

TABLE 8. *T* estimates at 10 kbar pressure

Sp. No.	Two-pyroxene		Garnet–clinopyroxene			Garnet–orthopyroxene			
	Wells	Davidson-Lindsley	Ellis-Green	Dahl	Krogh	Sen-Battacharya	Harley	Lee-Ganguly	Battacharya *et al.*
Mettuppalaiyam									
6D	811	1005	784	820	725	796	721	855	826
D87	846	1165	870	925	810	829	755	878	850
36M	791	957	758	705	684	892	798	934	893
40	-	-	-	-	-	748	674	785	788
P84	827	1078	-	-	-				
29F	-	-	689	636	619		-	-	-
P92C	-	-	796	850	740	-	-	-	-
P109	-	-	746	710	678	-	-	-	-
Kanjamalai									
14/M2	847	1013(21)	761	743	705	1038	892	1034	995
54	862	1055(20)	725	705	675	766	694	837	806
15/C	-	-	722	690	675	-	-	-	
14/O	-	-	843	768	817	-	-	-	-

Note: Dash indicates absence of the assemblage for the respective thermometer.

geothermometer (Sen and Bhattacharya, 1984; Harley, 1984*b*; Lee and Ganguly, 1988; Bhattacharya *et al.*, 1991).

The 2-px thermometer of Wells (1977) gave a limited temperature range (791–862°C). The temperature estimates (957–1078°C) obtained with the well-calibrated 2-px thermometer of Davidson and Lindsley (1985) are probably over-estimates because some of the clinopyroxenes contain more than 10% non-quadrilateral components. The results of grt–cpx thermometry are highly discordant and span the wide temperature range of 619–925°C for the various calibrations. Other calibrations of the grt–cpx thermometer (e.g. Pattison and Newton, 1989) give lower ranges of temperatures. The grt–cpx thermometers do not record the peak metamorphic temperature due to the low closure temperature for the Fe–Mg exchange between coexisting garnet and clinopyroxene (Frost and Chacko, 1989; Hensen, 1981). The discrepant results can also be due to the inadequate incorporation of non ideal solution properties of garnet and clinopyroxene in the various calibrations (e.g. Perkins, 1991). The various results of grt–opx thermometry are also highly inconsistent and span the temperature range 674–1038° for various calibrations. A consideration of the available solution models for garnet alone helps to explain these discrepancies. However, the latest calibration of the grt–opx thermometer by Bhattacharya *et al.* (1991) takes into account (i) reversed experimental data, (ii)

non ideal asymmetric mixing behaviour of Mg-Fe-Ca garnets, and (iii) non ideal Fe-Mg mixing in orthopyroxene. Thus, this calibration should yield the best estimates of temperatures. Moreover, the grt–opx pair may have a higher closure temperature than the grt–cpx pairs as it yields temperatures that are consistently higher than those yielded by the grt–cpx pairs. Nevertheless, within the framework of currently available geothermometers, accurate estimate of temperature of equilibration is not possible.

Pressure is chiefly calculated (Table 9) by (i) grt–opx geobarometer (Wood, 1974; Harley, 1984*a*) and (ii) grt–cpx geobarometer (Mukhopadhyay, 1991). Wood's (1974) version of the grt–opx geobarometer was updated by calculating the partial molar volumes of $Mg_2Si_2O_6$ and $MgAl_2SiO_6$ according to the molar volume data on aluminous Opx given by Danckwerth and Newton (1978). The grt–opx geobarometer yields highly inconsistent values of *P*, ranging from either 7–18 kbar (Harley's calibration, 1984*a*) or 5–16 kbar (Wood's calibration, 1974). The grt–cpx geobarometer, on the other yields quite consistent values of *P* (8 ± 1 kbar) for the Mettuppalaiyam samples in the temperature range of 850–900°. Similarly, for the Kanjamalai samples, the most consistent value of *P* is obtained as 12 kbar in the temperature range of 750–975°. For the two quartz-bearing samples, the geobarometer of Newton and Perkins (1982), based on the discontinuous reaction

TABLE 9. P estimates.

Sp. No.	Garnet–clinopyroxene Mukhopadhyay		Garnet–orthopyroxene Wood*	Garnet–clinopyroxene–plagioclase–quartz Harley	Newton-Perkins*
Mettuppalaiyam					
6D		7(900)	5(855)	7(820)	-
D87		8(900)	8(900)	10(850)	-
36M		8(850)	10(893)	15(893)	-
40		-	16(785)	18(785)	-
29F		9(850)	-	-	-
P92C		8(850)	-	-	-
P109		8(850)	-	-	-
Kanjamalai					
14/M2	12(750)	16(850)	11(995)	15(995)	16(761)
54	12(900)	15(975)	6(837)	7(805)	-
15/C	12(850)	16(975)	-	-	16(750)
14/O	8(850)	13(975)	-	-	-

Note: The numbers in parentheses give the temperature at which the pressure is estimated
Dash indicates absence of the assemblage for the respective barometer.
*Modified (see text)

$$CaMgSi_2O_6 + CaAl_2Si_2O_8 = 2/3\ Ca_3Al_2Si_3O_{12} +$$
$$1/3\ Mg_3Al_2Si_3O_{12} + SiO_2 \qquad (1)$$
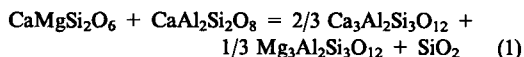
is also used (Table 9). This geobarometer depends on the presence of plagioclase and quartz (restricted to silica-over saturated rocks). The geobarometer of Mukhopadhyay (1991), based on the continuous reaction

$$CaMgSi_2O_6 + CaAl_2SiO_6 = 2/3\ Ca_3Al_2Si_3O_{12} +$$
$$1/3\ Mg_3Al_2Si_3O_{12} \qquad (2)$$
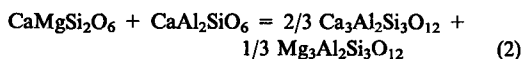
is analogous to (1) but does not depend on the presence of either plagioclase or quartz. For congruity, the activities of pyrope, grossular, and diopside in the basic formulation of the Newton-Perkins geobarometer (1982) were calculated according to the models used for the grt–cpx geobarometer (Mukhopadhyay, 1991). Application of the garnet-clinopyroxene-plagioclase–quartz geobarometer yields an equilibrium pressure of 16 kbar for both the silica over-saturated samples in the temperature range of 750–761°C. If the temperature is assumed to be in the range of 850–975°, then the grt–cpx geobarometer also yields 16 kbar pressure (Table 9). From the consideration of all these calculations we conclude that the Kanjamalai rocks reached a peak temperature of about 900 ± 50° in the pressure range of 14 ± 2 kbar, whereas the Mettuppalaiyam rocks reached a peak condition

of metamorphism at around 875 + 25° and 8 ± 1 kbar. Thus the two areas essentially lie along an adiabatic gradient.

Numerous studies have shown that granulite facies metamorphism generally occurs under conditions of $P_{H_2O} < P_{Total}$, i.e. under low a_{H_2O}. For the specimen 14/M2, a_{H_2O} is approximated by considering the end-member equilibrium

$$Ca_2Mg_5Si_8O_{22}(OH)_2 = 2\ CaMgSi_2O_6 +$$
$$1.5\ MgMgSi_2O_6 + SiO_2 + H_2O \qquad (3)$$
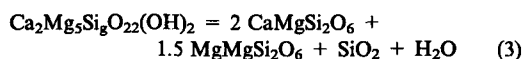
$\Delta H°$, $\Delta S°$, and $\Delta V°$ of this reaction are given by Welch and Pawley (1991). From these data, activity of water is calculated according to the following relationship

$$a_{H_2O} = \frac{-\Delta H^0}{RT} + \frac{\Delta S^0}{R} - \frac{(P-1)V^0}{RT} - \ln f_{H_2O} -$$

$$2\ln a^{Cpx}_{diopside} - 1.5\ln a^{Opx}_{enstatite} - \ln a^{Amph}_{tremolite} \qquad (4)$$

Activities of components in the solid phases are calculated by assuming ideal solutions (for approximation at least) and by adopting the mole fraction models given by Mukhopadhyay (1991) for the pyroxenes, and by Kohn and Spear (1989) for amphiboles (their Model 2). This calculation yields $a_{H_2O} = 0.78$. Although this supports the concept of metamorphism under conditions of $P_{H_2O} < P_{Total}$, this calculation

indicates a relatively H₂O-rich environment compared to the high CO_2-activity during the granulite facies metamorphism in south India that has been advocated by many workers (e.g. Janardhan et al., 1982; Santosh, 1987; Newton, 1990). The absence of similar assemblages in this study (two pyroxenes + amphibole + quartz) inhibits similar calculations for other samples.

Another important variable in metamorphism is f_{O_2}. Oxygen thermobarometer (Anderson and Lindsley, 1988) yields $T = 502°C$ and $\log f_{O_2} = -21.682$ at 8 kbar total pressure for the sample P92C [$\Delta \log f_{O_2} = 1.043$]. Similar low temperatures of $\sim 500°C$, determined with the two-oxide

thermometers, in other granulite facies terrains were interpreted by Frost and Chacko (1989) as due to resetting of the oxides at lower temperature. Coexistence of rutile and magnetite with ilmenite may also indicate reequilibration at a lower temperature (Lindsley, 1991). Coexistence of ilmenite and magnetite was not found in any other sample studied here (for sample 6D and 41/B estimation can not be performed because calculations yielded $T < 500°C$ which is outside the range recommended by Anderson and Lindsley, 1988). Although quantitative estimation of the extent of variation of f_{O_2} across the samples is not possible, the oxide thermometry indicates further reequili-
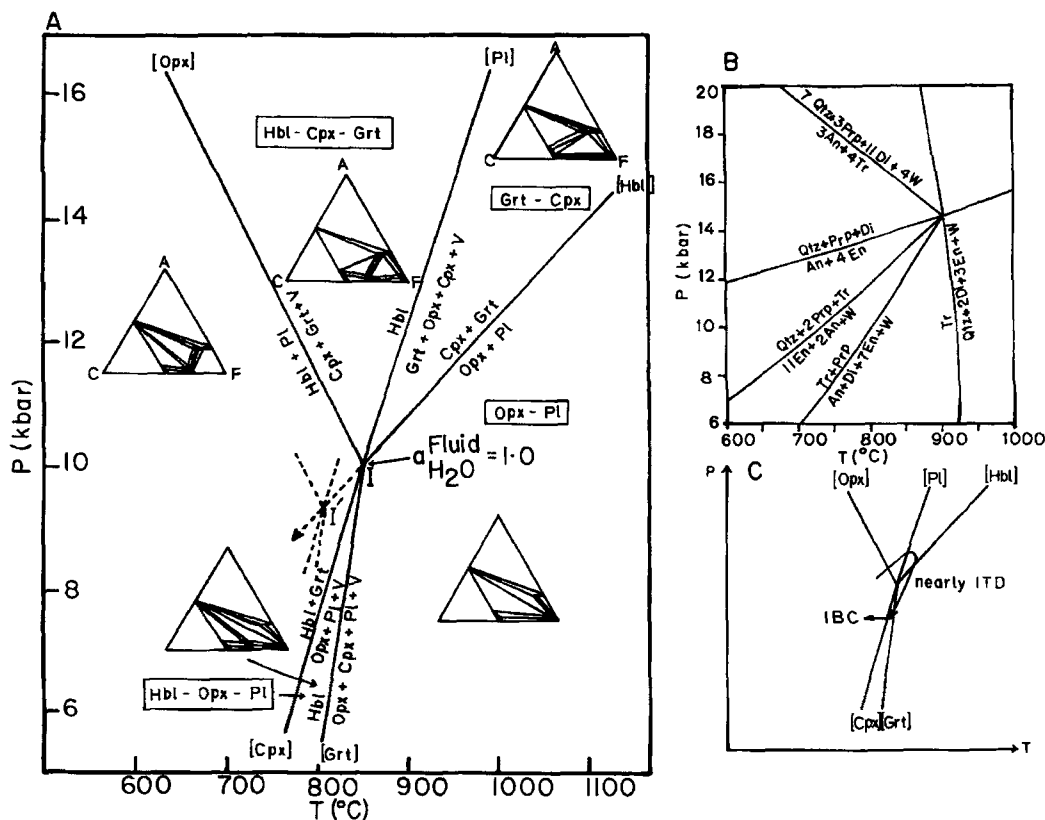
FIG. 8. (A) Schematic P–T grid showing possible equilibria involving the five dominant phases, viz. Cpx, Opx, Grt, Hbl, and Pl for fixed Fe/Mg ratios in the phases and a constant a_{SiO_2}. Phase compatibility triangles are shown with schematic representation of solid solutions according to Fig. 3. The different subfacies, represented by rectangular boxes are adopted from De Waard (1965b). (B). The schematic chemography, shown in (A) are calculated in the simple system CMASH from the thermodynamic data base of Berman (1988) to illustrate the idealized reactions and the general validity of the slopes and relative positions of the reactions shown in (A). (C). The clockwise P–T–t path (curved line with an arrow) of evolution of the mafic granulites of the Mettuppalaiyam-Kanjamalai areas in relation to the reactions shown in (A) and (B). Nearly ITD and IBC paths are explained in text.

bration during retrogression of the assemblages at a lower temperature than peak metamorphism.

Phase equilibria

The phase relations involving the five phases, Grt, Cpx, Opx, Hbl and Pl, is schematically illustrated with the aid of a P–T grid (Fig. 8A), The [Cpx] and [Opx] reactions, in general, define the onset of stable existence of hornblende–pyroxene granulites; the [Grt] and [Pl] reactions define the boundary between the hornblende–pyroxene granulite (hydrous facies) and anhydrous pyroxene granulites; and finally, the [Hbl] and [Opx] reactions mark the transition between the intermediate-pressure granulite, characterized by stable coexistence of Opx + Pl, and the high-pressure granulite (garnet-clinopyroxene subfacies) characterized by stable association of Grt + Cpx + Pl $\pm$ Qz (De Waard, 1965b; Sen and Ray, 1971b; Green and Ringwood, 1967; Hensen, 1981). For natural basaltic bulk compositions, the [Hbl] boundary, known as Grt-in reaction, was experimentally determined by Green and Ringwood (1967) and Ito and Kennedy (1971). In the simple system CaO–MgO–Al$_2$O$_3$–SiO$_2$ (CMAS) the reaction, written as

$4MgMgSi_2O_6 + CaAl_2Si_2O_8 =$
(orthoenstatite)   (anorthite)
$CaMgSi_2O_6 + \quad Mg_3Al_2Si_3O_{12} + SiO_2$ (5)
(diopside)   (pyrope)   (β-quartz)
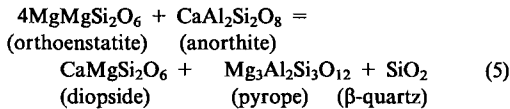
is valid for a quartz-saturated system and occurs at a much higher pressure than that shown in Fig. 8A (Hensen, 1981), and Fig. 8B). Green and Ringwood (1967) amply demonstrated the influence of Mg/(Mg + Fe^{2+}) ratio and SiO$_2$-content on the conditions under which garnet appears in basic rocks (Grt-in reaction). In SiO$_2$-undersaturated compositions, garnet appears at a much lower pressure, e.g. at 5 kbar at 800°C (data from Ito and Kennedy, 1971) than that necessary for SiO$_2$-saturated compositions. Low values of Mg/(Mg + Fe^{2+}) ratio in the bulk composition of the rock cause garnet to appear at lower pressure. Thus, for natural compositions, the exact location of the [Hbl] raction shown in Fig. 8 is subjective. The location of the [Grt] reaction is also dependent on the amphibole composition. In the simple system CMASH, the analogous reaction (Fig. 8B), given by (3) has been determined experimentally by Welch and Pawley (1991). For a natural hornblende composition (in olivine tholeiite) this amphibole-breakdown curve given by the appearance of Cpx, Opx, and Pl at the expense of amphibole with increasing temperature

was experimentally determined by Spear (1981). These low-pressure thermal breakdown curves of amphiboles are essentially temperature-dependent and hence have steep dP/dT slopes (Fig. 8A). Thus, the exact P–T coordinates of the invariant point (Fig. 8A) is subject to bulk chemical composition. Since. in each of the two cases, the samples are from a limited spatial distribution, it is postulated that these samples equilibrated around two invariant situations (Fig. 8), each characterizing a single locality. The P–T calculations indicate that such two invariant points should lie along an adiabat. Since the chief difference in the locations of two invariant points in the two different areas is P, this difference cannot be attributed to varying P_{H_2O} but to different bulk compositions. The invariant situation, I (Fig. 8A), assumes, $P_{H_2O} = P_{Total}$, a fixed Fe/Mg ratio, and constant a_{SiO_2}. In the event of variable a_{H_2O}, invariant point I will move along a univariant line toward I' for example, which indicates lowering of both P and T. Increasing the Fe/Mg ratio of the bulk composition should have a similar effect but if the rocks differ mainly in their SiO$_2$-content then high-pressure granulite assemblages develop in a varied bulk composition (e.g. no free quartz was found in the garnet–clinopyroxene granulites from Mettuppalaiyam) over a regional scale along an adiabatic P–T gradient. For the orthogneisses from South Harris, Wood (1975) also showed that it was not the Mg/(Mg + Fe^{2+}) ratio (which remained uniform) but the degree of silica saturation (or silica-activity, a_{SiO_2}) that was the prime factor in controlling the presence or absence of garnet. Granulite metamorphism (T = 800–860°; P = 9–13 kbar) produced Grt + Cpx + Pl assemblages in olivine-normative basaltic compositions and Opx + Cpx + Pl + Qz assemblages in quartz-normative rocks.

Our samples reveal the coexistence in close proximity of both hydrous and anhydrous assemblages as well as garnetiferous and nongarnetiferous assemblages (Fig. 2). These variations in a single locality however, can be partly due to variation in μ_{H_2O} between the layers and partly due to the difference in bulk chemical compositions (Fig. 8A). It is an intriguing problem to decipher which one of the two variables, μ_{H_2O} and bulk chemical composition, exert the dominant control on the observed variation in modal mineralogy. Bulk rock chemical analyses of samples 36M and 40 from Mettuppalaiyam show that there is virtually no significant chemical difference between these two samples. In the case of the Kanjamalai granulites, determination of fourteen bulk rock FeO/MgO shows that there is a complete overlap of this ratio in rocks of varied

assemblages. Similarly, the Mg#'s in various mineral phases do not follow any systematic modal mineralogy. Noted variation is found in terms of free quartz and anorthite content of plagioclase. Thus the question of whether the assemblages (1 and 2 above) are varied versions of a single member or are bulk compositional effects can be attributed to an interplay of μ_{H_2O} and a_{SiO_2}

P–T–t path and regional tectonics

The pressure–temperature–time path of the rocks is deciphered from a detailed analysis of textures (Harley, 1989) that were produced through crossing of univariant equilibria, depicted in Fig. 8. It has now been recognized that while the majority of the granulites exhibit clockwise (CW) P–T–t paths (P_{max} attained slightly after T_{max}) an anticlockwise (ACW) path (P_{max} attained slightly after T_{max}) is also manifested by many granulites (Bohlen, 1991). In the case of the Mettuppalaiyam–Kanjamalai granulites, the detection of the exact nature of the P–T–t path hinges critically upon two reactions vis. the hornblende breakdown reaction and the garnet producing reaction. The hornblende–pyroxene granulite, such as the assemblage Opx + Pl + Hbl ± Cpx, can be transformed to the pyroxene granulite (without hornblende) through crossing of the reaction [Grt]:

$$Hbl + Opx = Cpx + Pl \qquad (3')$$
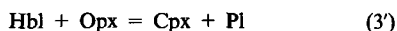
as postulated by many workers (e.g. Sen and Ray, 1971a,b), to be the key hornblende-breakdown reaction. Similarly, the garnet-producing reaction [Hbl]:

$$Opx + Pl = Cpx + Grt + Qz \qquad (5')$$

is believed to be responsible for the development of garnet + clinopyroxene in many garnet–pyroxene granulites from high-grade terrains such as those found in Sri Lanka (Schumacher et al., 1990). The possibilities described above, essentially suggests an ACW P–T–t path. However, a closer examination of the mineral textures reveals that the assemblages in the mafic granulites of both Mettuppalaiyam and Kanjamalai localities evolved along a CW P–T–t path (Fig. 8C). Even though the exact P–T trajectories in these locations are not identical, the basic qualitative nature of the two are the same. Figure 9 depicts the key textural features that help to establish the reactions responsible for the development of various assemblages. In the samples from Mettuppalaiyam, the rocks are generally polygonal (to interlobate) granoblastic

and garnet grains contain minor inclusions of hornblende, plagioclase, and clinopyroxene. In the Kanjamalai samples, garnets show a sieve texture with abundant inclusions of plagioclase, hornblende, and clinopyroxene. These suggest that garnet grew at the expense of plagioclase, hornblende, and possibly clinopyroxene. Thus there is abundant petrographic evidence to support the concept of formation of garnet through reaction [Opx] (Fig. 9A). Textural features also indicate that the reverse of reaction (5') produced the Hbl-free four-phase assemblages (Fig. 9B) implying a nearly isothermal decompression (ITD) path. In the garnet-free assembalges, hornblende contains abundant inclusions of orthopyroxene and plagioclase (Fig. 9C–F). This shows that the hydrous garnet-free assemblage developed through reaction [Cpx] and possibly reaction [Grt] also, from the high-pressure garnetiferous assemblage during an isobaric cooling (IBC) path. An effect of retrogression is also exemplified by development of secondary blue amphiboles from clinopyroxenes and in Sp. 40 secondary orthoamphibole around orthopyroxene. Thus, evolution of an essentially amphibolitic assemblage, Hbl + Pl + Cpx to a garnetiferous assemblage (Fig. 9G) through reaction [Opx], and development of the anhydrous garnet-clinopyroxene subfacies assemblages (Fig. 9I–J) from the five-phase invariant assemblage (Fig. 10H) through reactions [Pl] and [Hbl] suggest a CW P–T–t path with ITD implying tectonic thickening of the crust followed by exhumation. The basic granulites, discussed here, cannot be considered to be ancient in situ lower continental crust representing the granulite-eclogite transitional facies. The iron formations, associated with the metabasites were deposited in a platform area of shale, quartzite, and carbonates (Prasad et al., 1982; Subba Reddy and Prasad, 1982; Naqvi and Robers, 1987). This association indicates that the 'granulites' were related to a high pressure metamorphism which eventually could lead to the formation of eclogites by the deep burial of a supracrustal sequence (Fig. 10). The IBC was possibly related to the high H_2O activity during Proterozoic ductile shearinhg (Mukhopadhyay, 1986). The supracrustal sequence is confined within the Moyar-Bhavani and Noyal-Cauvery shear zone (Fig. 10) which are considered to be zones of crustal shortening (Drury and Holt, 1980; Drury et al. 1984). Eclogitization (dominantly garnet + omphacite clinopyroxene assemblage) of granulite-facies mafic rocks (dominantly garnet + aluminous clinopyroxene assemblages) along some shear zones in the Bergen arcs of Norway has been
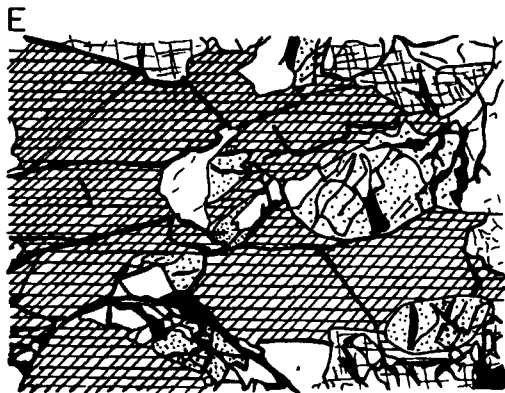
A

Hbl + Pl = Grt

B

Grt + Cpx = Opx + Pl

C

Opx + Cpx + Pl = Hbl

D

Opx + Pl = Hbl

E

Opx + Pl = Hbl

F

Cpx + Pl = Hbl

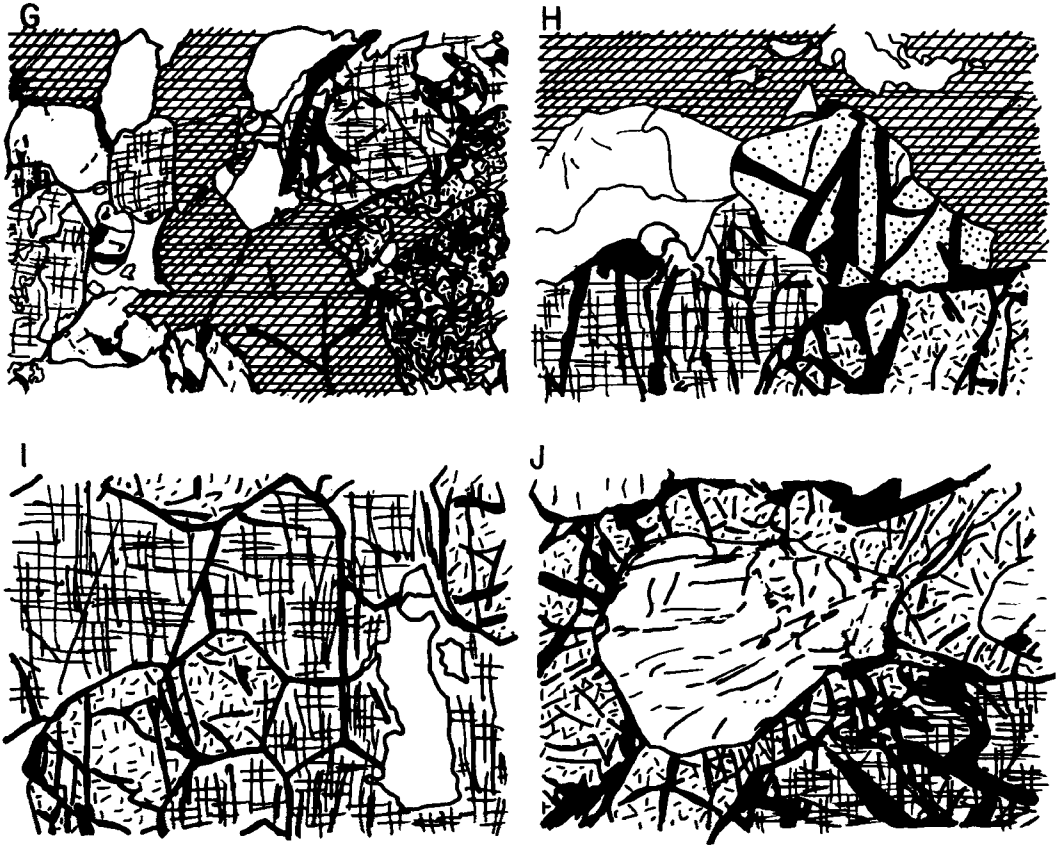▨ Grt   ▦ Opx   ▦ Cpx   ▭ Pl   ▨ Hbl

FIG. 9. Textural features of the granulites depicting key mineral reactions: (A) A hornblende pseudomorph comprised of remnant hornblende, plagioclase and orthopyroxene (only one grain) occurring in a large garnet porphyroblast indicating formation of garnet at the expense of Hbl and Pl. Opx perhaps developed later due to breakdown of Hbl. (B) Occurrence of Opx and Pl as interstital grains between Grt and Cpx indicate formation of the former two phases at the expense of the latter two. (C) Hbl crystals embay Opx, Cpx, and Pl indicating formation of Hbl at the expense of Opx, Cpx, and Pl. (D) Hbl crystals completely enclose Opx and Pl crystals indicating the reaction Opx + Pl = Hbl. (E) Same feature, as (D), is exhibited by all Grt-free samples. (F) In an Opx-free sample, Hbl encloses Cpx and Pl crystals. (G) In some samples, Hbl + Pl + Cpx rich portion grades into Grt-rich portion where Grt is very sieved containing Hbl and Pl crystals. (H) Five-phase equilibrium assemblage. (I) Polygonal, granoblastic mosaic texture involving coarse Grt and Cpx crystals and minor Pl crystals. (J) In some Grt-Cpx assemblages, Pl crystals are completely rimmed by Grt indicating Pl not at equilibrium with Grt and Cpx.

documented by Austrheim and Griffin (1985). This development of eclogite mineralogy at the expense of granulite facies minerals is attributed to a temporally latter increase in strain (deformation) that resulted in development of the shear zones (op. cit.). Apart from shear deformation, highly H_2O-rich ($X_{H_2O} > 0.75$) fluid infiltration along these shear zones was also considered to be

another dominant control in the transformation of granulites into eclogites (Austrheim, 1986; Jamtveit et al., 1990; Klaper, 1991). Thus, it can be postulated that the supracrustal sequence near the Moyar-Bhavani shear zone suffered an analogous strain and H_2O-rich fluid activity that resulted near eclogite-facies metamorphism in a granulite-facies environment.
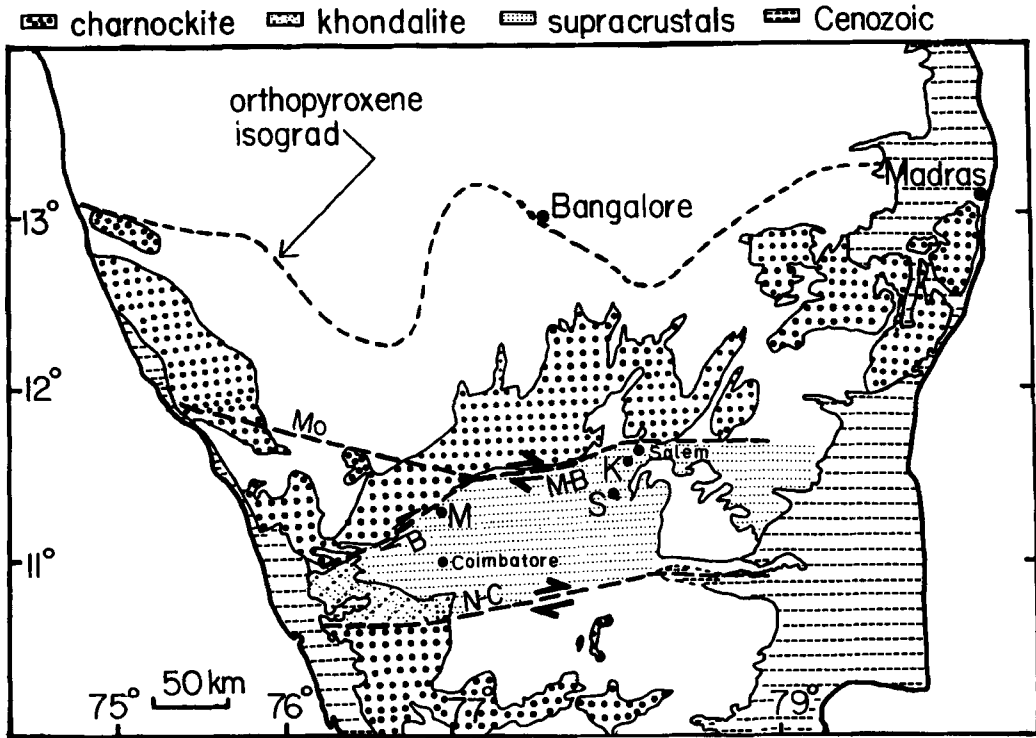
FIG. 10. Geological map of the part of the Precambrian granulite facies terrain of south India showing distribution of charnockites, khondalites, supracrustal sequences (shear complex), and Moyar (Mo), Bhavani (B), Moyar-Bhavani (MB), and Noyil-Cauvery (NC) shear zones in relation to the locations of Kanjamalai (K), Sittampundi (S), and Mettuppalaiyam (M) occurrences (Adapted from Fig. 1 of Raith et al., 1983 and Fig. 4.1 of Naqvi and Rogers, 1983). Also see Fig. 6 of Mukhopadhyay (1986).

Conclusions

Garnet–clinopyroxene and orthopyroxene–plagioclase subfacies basic granulites occur in close juxtaposition at Mettuppalaiyam and Kanjamalai along the Moyar-Bhavani shear zone of the high grade terrain of south India. Various attempts have been made to determine the $P-T$ conditions of granulite facies metamorphism in southern India (Newton and Hansen, 1986; Naqvi and Rogers, 1987). Most of the estimates are made for charnockites, and associated pelitic and/or meta-basic rocks. Raith et al.(1983) estimated T = 730–800°, P = 6.5–9.5 kbar for seven charnockitic occurrences in south India. Harris et al. (1982) recognized three fields of equilibration for the charnockitic and metapelitic assemblages: high-pressure granulites (P = 8.3 $\pm$ 1.0 kbar; T = 760 $\pm$ 40°C); medium-pressure granulites (P = 6.4 $\pm$ 1.0 kbar; T = 735 $\pm$ 40°C); and low-pressure granulites (P = 5.0 $\pm$ 1.0 kbar, T = 700 $\pm$ 20°C). The $P-T$ estimates of the type charnockite locality, as given by Bhattacharya and Sen (1986) are 6.5–7.5 kbar and 750–800°C. Two shear zones, viz. the northern Moyar-Bhavani and the southern Noyil-Cauvery shear zones, separate the medium-pressure granulites from the high-pressure granulites in the north and the low-pressure granulites to the south (Fig. 10). Newton and Hansen (1986) calculated P = 6–8 kbar and T = 700–750°C for the charnockite massifs of the high-pressure granulite regime of Harris et al. (1982). Thus, the $P-T$ conditions estimated for the basic granulites from Kanjamalai-Mettuppalaiyam area are higher than those obtained for most of the granulite-charnockite series of rocks from south India. These basic granulites reached almost the

extreme limit of granulite facies metamorphism where amphibole became unstable and eclogitic assemblages began to develop. Mineralogical characteristics suggest that the conditions of metamorphism did not attain the eclogite facies *sensu stricto*. For example, plagioclase is a ubiquitous phase and both the clinopyroxenes and the amphiboles are enriched in Tschermak's component relative to their jadeite contents and $Na^{B(M4)}$-site, respectively. Mineralogical characteristics, however, indicate a progression towards eclogite facies conditions. The difference in P conditions between the Mettuppalaiyam and Kanjamalai suites possibly indicates an adiabatic metamorphic gradient. Bulk rock chemical differences in terms of SiO_2 content can account for the development of similar mineral assemblages along this metamorphic gradient. At both of these places, the basic granulites occur in close association with BMQ, indicating a low-P protolith. The different mineralogies, garnet bearing and garnet-free samples, and hornblende-bearing and hornblende-free samples reflect a complex interplay of μ_{H_2O} and chemical variables notably, a_{SiO_2}, during high-pressure metamorphism. Because of the differences in bulk compositions, various reactions are arrested in different samples. These are detected by close examination of a variety of mineral textures which imply a CW P–T–t path during evolution of these granulites. This resulted from burial in a deep-seated condition by crustal thickening giving rise to near eclogite-facies assemblages in a variety of low pressure basaltic bulk compositions. An isobaric cooling accompanied later shearing and H_2O influx caused the development of the garnet-free assemblages.

Acknowledgements

References

Anderson, D. J. and Lindsley, D. H. (1988) *Amer. Mineral.*, **73**, 714–26.

Austrheim, H. (1986/87) *Earth Planet. Sci. Lett.*, **81**, 221–32.

Austrheim, H. and Griffin, W. L. (1985) *Chem. Geol.*, **50**, 267–81.

Berman, R. G. (1988) *J. Petrol.*, **29**, 445–522.

Bhattacharya, A. and Sen, S. K. (1986) *J. Petrol.*, **27**, 1119–41.

Bhattacharya, A., Krishnakumar, K., Raith, M., and Sen, S. K. (1991) *J. Petrol.*, **32**, 629–56.

Bohlen, S. R. (1991) *J. Metamorphic Geol.*, **9**, 223–9.

Bose, M. K. (1979) *Ind. J. Earth Sci.*, **6**, 200–19.

Cameron, M. and Papike, J. J. (1979) *Frotschr. Mineral.*, **57**, 28–67.

Chappel, B. W. and White, J. R. (1970) *Mineral. Mag.*, **37**, 555–60.

Condie, K. C., Allen, P. and Narayana, B. L. (1982) *Contrib. Mineral. Petrol.*, **81**, 157–67.

Dahl, P. E. (1980) *Amer. Mineral.*, **65**, 854–66.

Danckwerth, P. A. and Newton, R. C. (1978) *Contrib. Mineral. Petrol.*, **66**, 189–201.

Davidson, C. F. (1943) *Roy. Soc. Edinburgh Trans.*, **61**, 71–112.

Davidson, P. and Lindsley, D. H. (1985) *Contrib. Mineral. Petrol.*, **91**, 390–404.

De Waard, D. (1965a) *J. Petrol.*, **6**, 165–91.

De Waard, D. (1965b) *Amer. J. Sci.*, **263**, 455–61.

Drury, S. A. and Holt, R. W. (1980) *Tectonophys.*, **65**, T1–T15.

Drury, S. A., Harris, N. B. W., Holt, R. W., Reeves-Smith, G. J., and Wightman, R. T. (1984) *J. Geol.*, **92**, 3–20.

Ellis, D. J. and Green, D. H. (1979) *Contrib. Mineral. Petrol.*, **71**, 13–22.

Frost, B. R. and Chacko, T. (1989) *J. Geol.*, **97**, 435–50.

Green, D. H. and Ringwood, A. E. (1967) *Geochim. Cosmochim. Acta*, **31**, 767–833.

Harley, S. L. (1984a) *J. Petrol.*, **25**, 665–96.

Harley, S. L. (1989b) *Contrib. Mineral. Petrol.*, **86**, 359–73.

Harley, S. L. (1989) *Geol. Mag.*, **126**, 215–47.

Harris, N. B. W., Holt, R. W., and Drury, S. A. (1982) *J. Geol.*, **90**, 509–27.

Hawthorne, F. C. (1983) *Can. Mineral.*, **21**, 173–480.

Hensen, B. (1982) *Contrib. Mineral. Petrol.*, **76**, 234–42.

Howie, R. A. (1955) *Trans. Roy. Soc. Edinburgh*, **62**, 725–68.

Howie, R. A. and Subramaniam, A. P. (1957) *Mineral. Mag.*, **35**, 536.

Ito, K. and Kennedy, G. C. (1971) *Amer. Geophys. Union Geophys. Monograph*, **14**, 303–14.

Jamtveit, B. (1987) *Contrib. Mineral. Petrol.*, **95**, 82–99.

Jamtveit, B., Bucher-Nurminen, K., and Austrheim, H. (1990) *Contrib. Mineral. Petrol.*, **104**, 184–93.

Janardhan, A. S., Newton, R. C., and Hansen, E. C.

(1982) *Contrib. Mineral. Petrol.*, **79**, 130–49.

Klaper, E. M. (1991) *Schweiz. Mineral. Petrogr. Mitt.*, **71**, 231–41.

Kohn, M. J. and Spear, F. S. (1989) *Amer. Mineral.*, **74**, 77–84.

Kretz, R. (1983)*Ibid.*, **68**, 277–9.

Krogh, E. J. (1988) *Contr. Mineral. Petrol.*, **99**, 44–48.

Lee, H. Y. and Ganguly, J. (1988) *J. Petrol.*, **29**, 93–113.

Lindsley, D. H. (1991) *Rev. Miner.*, **25**, 69–128.

Lindsley, D. H. and Anderson, D. J. (1983) *J. Geophys. Res.*, **88**, A887–A906.

Livingstone, A. (1967) *Mineral. Mag.*, **36**, 380–8.

Lovering, J. F. and White, A. J. R. (1969) *Contrib. Mineral. Petrol.*, **21**, 9–52.

Morimoto, N., Fabries, J., Ferguson, A. K., Ginzburg, I. V., Ross, M., Seifer, F. A., and Zussman, J. (1988) *Amer. Mineral.*, **73**, 1123–33.

Mottana, A. (1986) *Lithos*, **19**, 171–86.

Mukhopadhyay, B. (1991) *Amer. Mineral.*, **76**, 512–29.

Mukhopadhyay, D. (1986) *J. Geol.*, **94**, 167–86

Naqvi, S. M. and Rogers, J. J. W. (1987) *Granulite terrain* Oxford Unversity Press, 82–101.

Newton, R. C. (1990) In: *Precambrian Continental Crust and Economic Resources (Naqvi, S. M. ed.)* *Elsevier, Amsterdam.*

Newton, R. C. and Hansen, E. C. (1986) In *The Nature of the Lower Continental Crust* (Dawson, J. B., Carswell, D. A., Hall., J., and Wedepohl, K. H., eds.) *Geol. Soc. Spec. Pub.*, **24**, 297–307.

Newton, R. C. and Perkins III, D. (1982) *Amer. Mineral.*, **67**, 203–22.

Pattison, D. R. M. and Newton, R. C. (1989) *Contrib. Mineral. Petrol.* **101**, 87–103.

Perkins, D. (1991) *Geol. Soc. Amer. Abst. Pro.*, **23**, 392–93.

Prasad, C. V. R. K., Subba Reddy, N., and Newton, R. C. (1989) *Contrib. Mineral. Petrol.*, **101**, 87–103.

Raith, M., Raase, P., Ackermand, D., and Lal, R. K. (1983) *Roy. Soc. Edinburgh Earth Sci. Trans.*, **73**, 221–44.

Ramberg, H. (1984) *Econ. Geol.*, **43**, 553–70.

Ray, S. (1970) *Neues Jahrb. Mineral., Mh.*, 456–66.

Ray, S. and Sen, S. K. (1970) *Neues Jahrb. Mineral., Abh.*, **114**, 61–88.

Robinson, P., Spear, F. S., Schumacher, J. C., Laird, J., Klein, C., Evans, B., and Doolan, B. (1982) *Rev. Mineral.*, **9B**, 1–228.

Santosh, M. (1987) *Contrib. Mineral. Petrol.*, **93**, 343–56.

Saravanan, S. (1960) *Ind. Miner.*, **1**, 69–84.

Schumacher, R., Schenk, V., Raase, P., and Vitange, P. W. (1990) In *High-grade metamorphism and Crustal Anatexis*, (Ashworth, J. R. and Brown, M., eds.) Allan & Unwin, London.

Sen, S. K. (1973) *Contrib. Mineral. Petrol.*, **38**, 299–306.

Sen, S. K. and Bhattacharya, A. (1984) *Contrib. Mineral. Petrol.*, **88**, 64–71.

Sen, S. K. and Ray, S. (1971a) *Neues Jahrb. Mineral., Abh.*, **114**, 301–19.

Sen, S. K. and Ray, S. (1971b) *Neues Jahrb. Mineral., Abh.*, **115**, 291–314.

Spear, F. S. (1981) *Amer. J. Sci.*, **281**, 697–734.

Subramaniam, A. P. (1956) *Bull. Geol. Soc. Amer.*, **67**, 317–379.

Subramaniam, A. P. (1956) *Bull. Geol. Soc. Amer.*, **67**, 317–379.

Subramaniam, A. P. (1959) *Amer. J. Sci.*, **257**, 321–53.

Subba Reddy, N. and Prasad, C. V. R. K. (1982) *J. Geol. Soc. Ind.*, **23**, 80–84.

Viswanathan, T. V. (1969) *Geol. Ind. Mem.*, **100**, 37–66.

Weaver, B. L., Tarney, J., Windley, B. F., Sugavanam, E. B., and Venkata Rao, V. (1978) In *Archaean Geochemistry* (Windley, B. F., and Naqvi, S. M., eds.) Elsevier, 177–204.

Welch, M. D. and Pawley, A. R. (1991) *Amer. Mineral.*, **76**, 1931–1939.

Wells, P. R. A. (1977) *Contrib. Mineral. Petrol.* **62**, 129–139.

Windley, B. F. and Selvan, T. A. (1975) *J. Geol. Soc. Ind.*, **16**, 209–215.

Wood, B. J. (1974) *Contrib. Mineral. Petrol.*, **46**, 1–15.

Wood, B. J. (1975) *Earth Planet. Sci. Lett.*, **26**, 299–311.